Time Dilation Visualization in Relativity

Ping-Kang Hsiung*
Robert H. Thibadeau†
Christopher B. Cox‡
Robert H. P. Dunn§

Carnegie Mellon University
Pittsburgh, Pennsylvania 15213

Abstract

This work extends our previous effort in visualizing the spatial aspect of relativistic effects, and treats the phenomenon of time dilation; an inherent temporal effect of special relativity.

Here, we demonstrate through still-frame images and live animations that in *observing* the viewing independent time dilation, the finite light transit time involved in performing the observation makes the *observed* time dilation also depend on the viewing condition.

As we introduce the physics of special relativity into ray-tracing and make time to pass as a ray travels through space, we are able to link the spatial and temporal dimensions in a fundamental and consistent way in our simulations, and generate images that reveal the spatial *and* temporal properties of the 4D geometry of *spacetime*.

Our exploration highlights the interplay of the imag*ing* process and the imag*ed* physical events in producing the final images. It reveals a richly detailed physical reality which the mathematical language of *thought experiment* in relativity does not directly provide.

1 Introduction

In this work we study the temporal phenomenon of time dilation in special relativity. This is a continuation of our previous effort[3] which focused on visualizing the spatial distortions of special relativity.

*Department of Electrical and Computer Engineering, Carnegie Mellon University. (412) 268-2524. pkh@cs.cmu.edu

†Imaging Systems Laboratory, The Robotics Institute, Carnegie Mellon University. rht@vi.ri.cmu.edu

‡Department of Physics, Carnegie Mellon University.

§Department of Art, Carnegie Mellon University.

This research was partially supported by Imaging Systems Laboratory, The Robotics Institute, Carnegie Mellon University.

Time dilation is evident in the following way: the progress of time slows down as the time-keeping device undergo relative motion. A manifestation of this physical model is that an atomic clock on a high speed spacecraft ticks slower than a clock at ground control from the view point of the latter. The scale of the slow-down depends solely on the motion speed: the faster the spacecraft moves, the slower its clock ticks relative to the ground.

In observing time dilation, however, the change of time scale appears to depend on the viewing angle as well as the speed. This additional, viewing dependent factor comes from the finite time of flight (TOF) of light, and is inevitably introduced as we use light to communicate the temporal information between the fast traveling object and the observer (camera).

Both time dilation and the TOF factor are natural phenomena in a universe simulated with rays of finite speed. When the physics of special relativity is brought into ray-tracing and when time is made to pass as a ray travels through space, the spatial and temporal dimensions are linked in a fundamental way, and both time dilation and the TOF element appear to be the built-in properties of the 4D geometry of spacetime.

In the following, we briefly review the relativity physics of time dilation and the TOF, and examine our relativistic ray-tracing technique. We then present our approach in visualizing the relativistic temporal effect and show the results.

2 Background

2.1 Spacetime physics

There are two principles in Einstein's special theory of relativity (1905) [11][12][8]:

1. Physical laws must be the same for observers in all inertial reference systems.[1]

[1] Also referred to as *inertial frames* or, in short, *frames*. A reference system is *inertial* if it is nonaccelerating.

CH2916-5/90/0000/0835/$01.00 © IEEE

2. Light speed is a constant as measured in all frames, and is independent of the light source motion relative to the observer.

When a physical event is measured, all frames have to record their individually defined space *and* time measurements. Among the frames, the different measurements are related by the Lorentz Transformation.

2.1.1 Time dilation

For two frames in relative motion, their time scales differ; judging from each frame, the rate time progresses in the other frame (the "moving frame" time) is slower than that of its own. This is the effect of time dilation, and is modeled in the Lorentz Transformation[8], from which one can derive the following equation:

$$\Delta t = \gamma \Delta t' \quad (1)$$

$\gamma = 1/\sqrt{1 - \| \vec{\beta} \|^2}$. $\| \vec{\beta} \|$ is the magnitude of the relative motion velocity $\vec{\beta}$.[2]

Equation 1 states that a time period $\Delta t'$ of a clock at rest in frame S' is measured to be γ times slower ($\gamma \Delta t'$) in a frame S when S' is in motion relative to S.[3]

Conceptually, for a lighthouse that is flying at 0.99c with respect to the ground, time progresses slower relative to a supervisor on the ground.

Note that the dilation factor γ depends solely on the relative motion speed, and evaluates to a larger number for a higher speed.

2.1.2 The "time of flight" of light

Adding to the complexity of the above, when one attempts to *observe* the time dilation of a moving clock through communication of light signals from the clock frame to the observation frame — e.g. sending two light pulses to mark the beginning and end of a time period of, say, one second — the non-zero time of flight necessary for light pulses to travel between the frames introduces an additional temporal factor. As the light-sending source is moving at a speed comparable to that of the light being sent, a phenomenon similar to the Doppler effect in sound occurs; wavefronts pile up densely in front of the moving source, and spread out more sparsely behind the source. This makes the *observed* dilation also depend on the angle between the receiving direction and the motion direction [8]:

$$\Delta t = (1 + \vec{e} \cdot \vec{\beta}) \gamma \Delta t' \quad (2)$$

in which $\vec{e}$ is the unit vector in the receiving direction from the view of the receiver. Note that when the source is perceived at the exact sideways viewing condition, we see the "pure" time dilation — when $\vec{e} \cdot \vec{\beta} = 0$, equation 2 becomes equation 1.

Conceptually, the supervisor on the ground becomes aggravated when he looks at the flying lighthouse and sees that it blinks at a *varying* rate.

2.2 Related work: ray-tracing relativity

When the scene objects and the image plane (the camera plate) are in relative motion at speeds comparable to light-speed, the time information must be interwoven with the spatial coordinates in defining the image formation process. Our work on the *REST-frame* relativistic ray-tracer[3][5][6] incorporates the finite light-speed and the relativity physics in ray-tracing. Rays are fired from the camera point at the imaging time, and travel backward in 4D spacetime to their source events in the past.

2.2.1 How to put special relativity into ray-tracing

In REST-frame, the image formation event is defined to take place at the spacetime point[4] $[x_0, y_0, z_0, t_0]$ in frame S (the "camera frame"), in which the image plane is stationary. For all objects that are in motion at the same speed relative to the camera frame S, we can find an object proper frame S' that satisfies some axes alignment conditions (see [3]). We can fire screen rays as defined in S frame by the camera parameters, and transform the rays to their S' representations. The new rays can then be tested against the stationary objects in S' for intersections (figure 1) based on the conventional ray-tracing technique [9][2][1].

After a ray hits an object in the object's proper frame, the time of flight is calculated between the ray origin and the hit point to determine the hit time. Together the hit point and the hit time forms the spacetime hit event. It is both geometrically visible, in the conventional ray-tracing sense, and *temporally* visible from the ray origin. New rays are spawned at this hit event using the hit event as the new rays origins. The new ray directions are determined by applying reflection and refraction laws in classical optics in the proper frame of the hit object.

In summary, we "freeze" objects in their proper frame and perform conventional ray-object intersection tests in the proper frame, with the additional calculation of the time passage as each ray travels through space.

[2] $\vec{\beta}$ is the velocity expressed in the unit of light-speed c. See [8][3].

[3] The S' in which the clock is stationary is called the *rest frame* or *proper frame* of the clock, and $\Delta t'$ taken in S' is referred to as the *proper time* of the clock.

[4] We use the symbol (x, y, z) for 3D positional coordinates and $[x, y, z, t]$ for a spacetime event point. When we designate a specific reference frame S, we use $(x, y, z)_S$ and $[x, y, z, t]_S$. Individually, each component is written with a subscript S (e.g. t_S). We also use $[x_0, y_0, z_0, t_0]_S$ as a shorthand for event $[x(t_0), y(t_0), z(t_0), t_0]$, and $(x_0, y_0, z_0)_S$ for $(x(t_0), y(t_0), z(t_0))$.

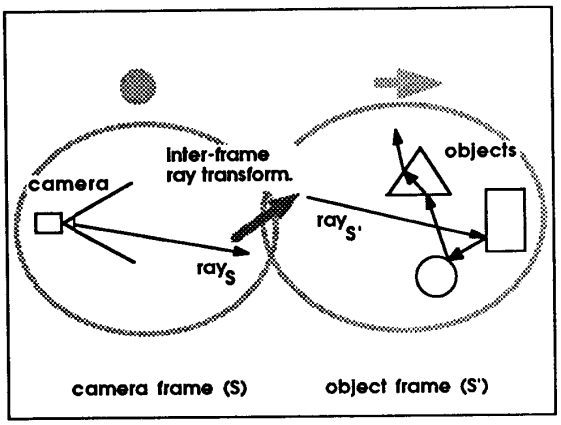

Figure 1: Ray transformation and proper frame ray-object intersection test.

2.2.2 Multiple object velocities

In the most general case, the objects are moving at different velocities.[5] We can establish multiple proper frames $S'_1, S'_2, ..., S'_n$, one for each object or group of objects that travels at a unique velocity. For the ray-object intersection computation, we transform a ray from the frame the ray is formed to all existing frames, and perform in each frame intersection tests between the transformed ray and the objects in the frame. If the ray hits objects in more than one frame, we sort the hit events in time order in one frame; most naturally, this can be done in the ray origin frame. The most *recent* event from the ray origin is identified as the true hit (figure 2).

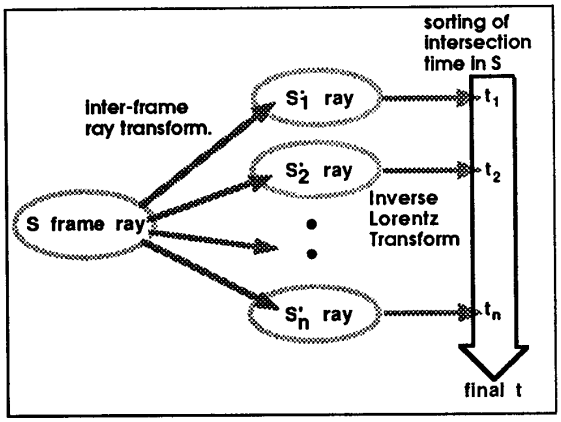

Figure 2: Multiple frame intersection and time sort.

[5]See [4]. The light sources can also attain various velocities.

3 Problems in visualizing time

There are some obstacles in attempting to *visualize* time dilation. Firstly, time is not visible in scientific or non-scientific senses. On the human intuition level, our perception of "time passes" is not regular. In physics, time is taken as the given foundation to measure everything else. In experiments, values for variables such as velocity are determined based on a prior knowledge of time interval. Still-frame images, stroboscopic photography (figure 3) and motion blur effects (figure 4) show how *fast* an object moves relatively, rather than the time component involved.[6] In both figures, the speeds of the spheres are: 0.99c for the top, 0.9c for the bottom, and stationary for the center. The top sphere is obviously the fastest judging by the longest distance it travels during the imaging time interval.

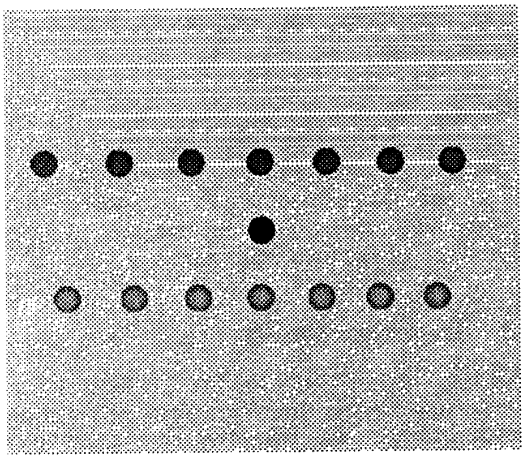

Figure 3: Multiple exposure view of fast moving spheres (7 exposures evenly spaced in a 6 second interval).

Also, restoring temporal sense to multiple time scales, which are non-linearly related, in a direct, visual, and most importantly, experiential manner requires innovative designs.

4 Approach and Implementation

The flying lighthouse in section 2.1 is a telltale example of our approach. We assign a periodic temporal definition to an object in its proper frame, and animate the object from the observation frame, relative to which the object moves. Using REST-frame to generate the animations, we can literally *see* the combined temporal effect of time

[6]Consider that the same motion blur can be created from two objects moving at different speeds by using two different exposure intervals.

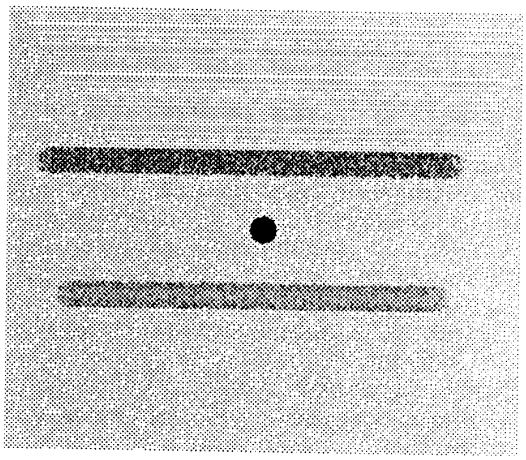

Figure 4: Fast moving spheres imaged with motion blur (6 second interval).

dilation and the time of flight of light, in the form of the increased or decreased temporal evolution of the object.

Multiple-exposures can be used in combination with temporal definition to illustrate time variation in still frame images, and objects moving at different relativistic velocities can be shown together for contrast.

4.1 Time visualization

This approach overcomes the time visibility problems stated in section 3 in the following manner: In experimental science, time is defined by the counts of certain atom vibrations. With the help of an imaginary "*space-time magnifier*" that scales down the high frequency counts in addition to scaling up the spatial dimensions (as an advanced scanning microscope does), we can imagine *seeing* "time passes" as the magnified time-keeping atom happily blinks away — one flash marks one second, for instance.

At our perception level, as time passes while we view the animation, the apparent variation of objects is mapped to our internal sense of time, and interpreted perceptually as a temporal variation. When we animate at real-time, the visual image of a blinking atom (or a lighthouse) can be received as a time-keeping device. Multiple blinking objects of various relativistic speeds can be imaged at once from one observation frame, and experienced by an animation viewer, whose internal temporal reference is naturally attached to the observation frame time, as to be keeping various time scales and blinking at different rates.

It is worth mentioning that blinking of objects also functions as synchronization signals between frames — in the tradition of thought experiment in relativity — and serves true physical purposes. In short, how do we measure time that is progressing in a different frame? Well, we have the frame tell us about it, e.g. by sending us a periodic radio or light signal.

4.2 The blinking rate equation

As we intend to observe the change of blinking *rates*, it is more useful to rewrite equation 2 as a frequency relation:[7]

$$f = \frac{1}{(1+\vec{e}\cdot\vec{\beta})\gamma} f' \triangleq \alpha f' \qquad (3)$$

That is, a proper frame blinking rate of f' is observed in the camera frame to be α times faster/slower.

Figure 5 shows the graphs of the viewing dependent factor α in equation 3 evaluated at speeds 0.85c, 0.9c and 0.99c. The horizontal axis is the viewing direction enumerated from $-90°$ to $90°$ in the camera frame, with $-90°$ being the object approaching and $90°$ being receding. At $0°$, the viewing direction is exactly perpendicular to the object motion direction (i.e. object is viewed to be in transverse motion.) The vertical axis is the *observed* frequency change factor α. The factor for the 0.99c curve at $-90°$ is 14.1.

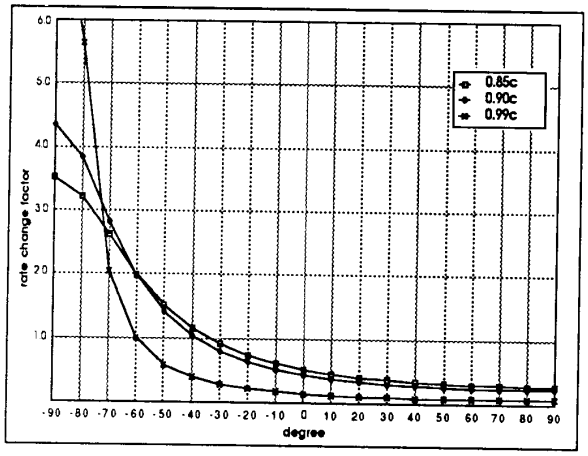

Figure 5: Viewed frequency variation factor versus viewing direction.

In observing time dilation, we expect, based on figure 5, to observe the relativistic temporal effect as the combination of time dilation and the time of flight of light during almost the entire course in which a blinking source approaches us from afar ($-90°$) in the beginning, and recedes from us ($90°$) at the end. The viewed blinking rate is the highest at the beginning, and the lowest at the end. In this graph, the "pure" time dilation is seen when the source is perceived at the exact sideways viewing condition ($0°$).

[7] This is the same equation that governs the *relativistic Doppler shift*, as the finite light transit time is the basis for both effects.

Another special viewing angle is when the factor becomes unity (1.0). This is the "cross-over" angle at which the source is momentarily seen to blink at its proper frame rate. Note that the faster the object moves, the "earlier" it reaches the cross-over angle.

4.3 Temporal variation detection

In making an object "blink", we assume the entire object is capable of changing color *instantaneously* and *simultaneously* according to a periodic color function in time *defined in its proper frame.*[8] A blue ball that flashes yellow for the duration of 0.5 seconds in every second, beginning on the second in its proper frame, is defined in the input file as:

```
% period 1.0
% interval 0 0.5 Yellow
% interval 0.5 1.0 Blue
```

period specifies the duration (in seconds) of one full cycle of color change, and each *interval* lists an individual color and its corresponding activating interval in a cycle. More complex repetition patterns can be defined similarly.

The color function of each object is stored with the object for the shading computation in ray-tracing. When a ray hits an object in frame S_i', the hit time in frame S_i', $\bar{t}_{S_i'}$, is derived from the hit distance (the distance between the hit point and the spatial part of the ray origin in S_i') and the ray origin time in S_i':

$$\bar{t}_{S_i'} = t_{ray.ori_{S_i'}} - \frac{d_{S_i'}}{c} \qquad (4)$$

The hit distance $d_{S_i'}$ is, conveniently, the intersection parameter returned by the intersection routine of almost every ray-tracer. The hit time $\bar{t}_{S_i'}$ is then used to evaluate the object's color *at that time*, as the the color function is also defined in the object's proper frame.

This temporal property evaluation mechanism handles the finite "time-of-flight" in spacetime in an implicit yet comprehensible manner: the ever-changing flight time for consecutive wave fronts traveling from a moving light source to the observer — the effect that results in the dilation factor variation that equation 2 (or equation 3) models — is consistently accounted for in the process of tracing the finite speed rays through spacetime and determining the time component of a hit point using equation 4. The latter is essential in keeping the spacetime consistency of the REST-frame simulation.

Obviously, the passage of time is the central scheme for a finite light-speed ray-tracer; space and time are integrated as a ray moves through spatial points and disseminates the time information along its propagation path.

[8]Simultaneity in *one* frame is a "valid" concept in relativity.

4.4 Camera control in spacetime animation

One final tool in making spacetime animations is the *object tracking* technique: an algorithm to pan the camera in spacetime to keep the moving objects "locked on" to the central part of the screen.

In the conventional animation, panning the camera (or, controlling the camera orientation) in 3D is done via controlling the camera "look-at" point: The object point to be tracked is assigned to be the camera look-at point. This makes the camera axis pass the tracked point, with the effect that the tracked point shows up at the center of the synthesized images.

Here, a tracked point is a 4D event, and tracking it is not an intuitive task because the camera orientation needs to be programmed to follow the objects as they move through spacetime, taking into account that 1) space appears to be *anisotropically* contracted due to relative motion, and 2) finite light-speed requires camera to capture those photons emitted from objects at their certain past.

The tracking problem and its solution can be formulated as follows:

Problem: Given the camera event $[x_{from}, y_{from}, z_{from}, t_{from}]_S$ and the target spatial point in S', $(x_{track}, y_{track}, z_{track})_{S'}$. Find the camera axis orientation in S so that the target spatial point appears at the center of the image plate.

Solution: The camera orientation is defined by a spatial look-at point *in S*, $(x_{at}, y_{at}, z_{at})_S$. The following algorithm produces a look-at point that satisfies the tracking requirement:

1. Convert the camera event in S, $[x_{from}, y_{from}, z_{from}, t_{from}]_S$, to S' using the Lorentz Transformation.
2. Find the time difference $\Delta t_{S'}$ between $\vec{X}_{from_{S'}} = (x_{from}, y_{from}, z_{from})_{S'}$ and $\vec{X}_{track_{S'}} = (x_{track}, y_{track}, z_{track})_{S'}$. When c is set to 1, this is the 3D *spatial* distance between $\vec{X}_{from_{S'}}$ and $\vec{X}_{track_{S'}}$.
3. Set $t_{track_{S'}} = (t_{from_{S'}} - \Delta t_{S'})$. This utilizes the fact that in S', in order for spatial point $X_{track_{S'}}$ to show up on the camera placed at $\vec{X}_{from_{S'}}$ at time $t_{from_{S'}}$, the photons have to be emitted[9] from $\vec{X}_{track_{S'}}$ at time $(t_{from_{S'}} - \Delta t_{S'})$.
4. Convert the target event $[x_{track}, y_{track}, z_{track}, t_{track}]_{S'}$ back to the camera frame. The spatial coordinates are the components of the camera look-at point $\vec{X}_{at_S} = (x_{at}, y_{at}, z_{at})_S$.

With this tracking technique, we can integrate the separate animation sequences of approaching objects, transversely moving objects and receding objects into a continuous animation.

[9]Notice that in S', $\vec{X}_{track_{S'}}$ is a stationary point in space, whereas $\vec{X}_{from_{S'}}$ changes with time.

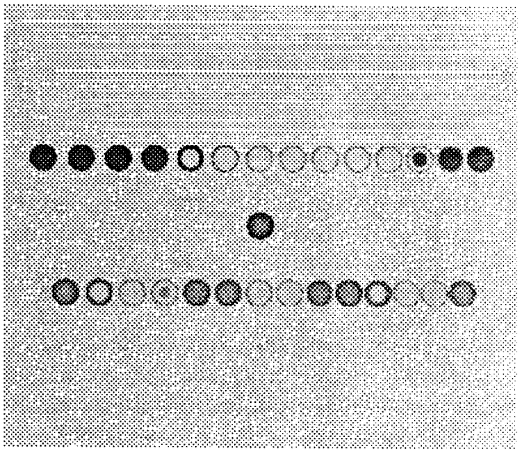

Figure 6: Multiple-exposure view of moving blinking spheres (0.5 second imaging intervals).

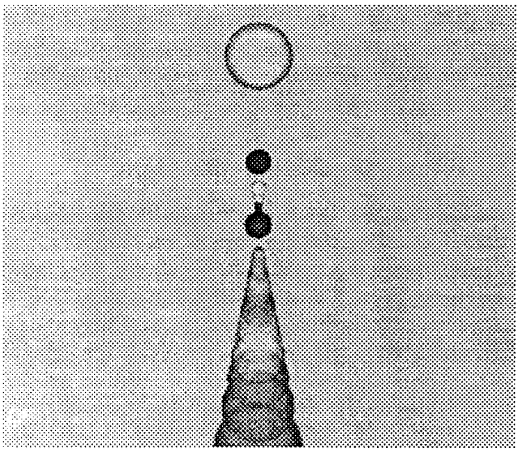

Figure 7: Approaching blinking spheres (0.2 second imaging intervals).

5 Experiments

We have implemented the spacetime software discussed in the previous section. Animations that demonstrate the visualization of time dilation have been successfully produced using the software. In the following, we present images that highlight our animation work.

We have chosen to use spheres in most of our illustrations. Besides their being easy to model and inexpensive to render, the major consideration we had was that objects of all other geometric shapes undergo distortion when imaged moving fast[3][4][7]; spheres, however, maintain their spherical outlines under such a condition.[10] The deformation in shape, visually exciting as it is, may be distracting as it is independent of the illustrated subject.

5.1 Conventions

For the clarity of our demonstrations, we used the following conventions consistently throughout our scene modeling and image generation:

1. **Color represents speed:** Red spheres are the fastest, and travel at 0.99c; green spheres travel at 0.9c, brown spheres at 0.85c, and blue spheres stationary. These speeds correspond to the γ values of 7.089, 2.294, 1.898 and 1.

2. **One Hertz blinking rate:** Each sphere turns to color yellow (blinks yellow) for 0.5 seconds in every second in its proper frame, and attains its original color (red, green, brown or blue) for the other 0.5 seconds. The change-over between colors is assumed to be instantaneous.[11]

3. **Realtime (Normal speed) animation and replay:** All animations are simulated in true time scale and recorded at the same pace. When they are played-back, the time frame of the viewer *is* the time of the camera frame (a second for a second); any temporal slow-down or speed-up of events observed by the viewer reflects the accurate, un-altered change in the evolution rate. Multiple-exposure images in this paper are *uniformly* exposed (sampled) at rates indicated with the images.

Also note that the Doppler color shift is not modeled in our images.

5.2 Images

5.2.1 Blinking spheres

In figure 6, three blinking spheres are imaged with a multiple-exposure view. The exposures are separated by 0.5 second intervals in the camera frame. The moving spheres (top and bottom, red at 0.99c, green at 0.9c) are approximately transverse with respect to the camera viewing direction, and thus exhibit the "pure" time dilation (blink at once per 7.09 and 2.29 seconds, respectively, in the camera frame).

In figure 7, the two moving spheres (red and green) are imaged to approach the camera while blinking at 1 Hz in

[10] See Penrose[10]. It was shown mathematically that a sphere in relativistic motion appears to have its surface "sheared", but remains to have an overall spherical outline.

[11] The imaging time is also instantaneous unless stated otherwise. Although neither assumption about instantaneity is essential, they bring down the image generation time.

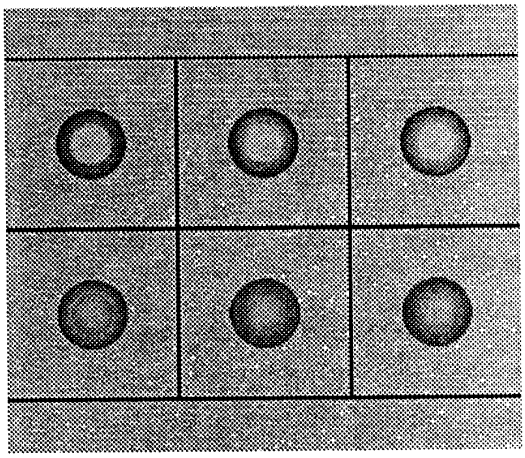

Figure 8: The "rings" due to the finite light-speed.

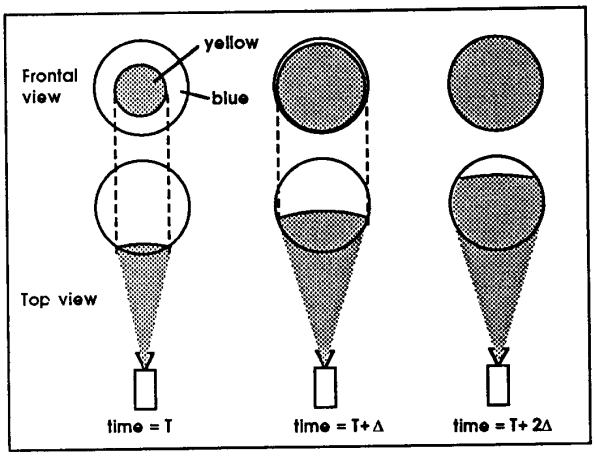

Figure 9: Illustration of the cause of the ring effect.

their individual proper frames. In the camera frame, they are predicated by equation 2 (also see figure 5) to blink at approximately 14.1 Hz and 4.36 Hz. The interval between consecutive exposures is 1/5 second, and thus is unable to sample correctly the 14.1 Hz blink of the red sphere. Using a higher sample rate, 1/30 for instance, differentiates the red blinks but makes the images of the green sphere overlay too closely.

In figure 8, we show one effect of finite light-speed on an object distributed in a large region — a peculiar visual phenomenon occurs as photons emitted from objects at different times in the past arrive at the camera plate concurrently, owing to the different distances they travel. In this figure, a stationary blinking sphere is viewed changing its color from blue to yellow (upper row) and from yellow back to blue (lower row). The change of color is programmed to occur simultaneously, but is viewed to occur like an expanding "ring" (or disc). At each moment, wavefronts belonging to the most recent blinks in the past are viewed to propagate outward on the sphere surface as concentric yellow rings. The central point on the sphere, being the closest point to the camera, appears to be the center and the origin of the out-bound rings. Figure 9 illustrates this in three time steps.

In fact, the "ring effect" can also be seen in the motion of smaller spheres. What is needed is to increase the temporal sampling rate of the multiple-exposure imaging. Figure 10 is produced by using the same configuration as figure 6, but doubling the sampling rate to 4 times per second.

Another phenomenon[12] related to the finite light-speed is that a row of (stationary) spheres blinking synchronously will appear to be out of step when viewed from a camera place at some distance away.

[12]We show this in our animations.

5.2.2 Blinking lattice

Figure 11 shows a blinking 3D lattice at rest. The lattice is made up of rods joined by spherical balls; it has a rectilinear structure: the rods are straight, and they meet at 90-degree angles. The entire lattice blinks simultaneously in its proper frame. This images exhibits the "ring effect" in *three dimensions*.

Figures 11 through 17 demonstrate the intriguing connection between the temporal and spatial aspects of relativistic imaging. In these time sequence images, the blinking 3D lattice is made to move towards the camera at 0.99c. In figure 11 the camera is placed at the central axis of the lattice. In figures 13 through 17, the camera is placed slightly to the right of the central axis of the lattice.

The consecutive images are 0.1 seconds apart in the camera frame. The effects that can be seen in these snapshots include the propagation of wavefronts as rings in space, the Lorentz-Fitzgerald length contraction in the direction of motion, the hyperbolic warping of the 3D grid, the apparent "rotation" (the *Penrose rotation*) of objects, and the increased blinking rate viewed in the camera frame. Note the seemingly "impossible" angle of the reflection on the right frontal sphere due to Penrose rotation.

6 Possible extensions

We expect to extend our scheme of temporal rules assignment to include the assignment of piecewise linear or analytical functions to objects. Objects will then change their colors gradually as time evolves. This extended view will also allow some other concepts and scenarios to be introduced into our simulations. For instance, a capability for time-modulated change of color (frequencies) as well

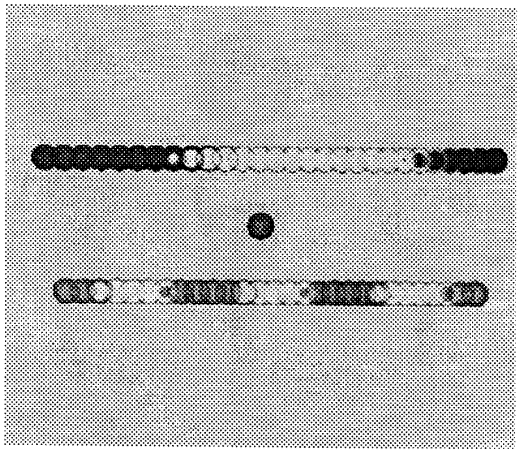

Figure 10: The "ring effect" as seen on smaller spheres.

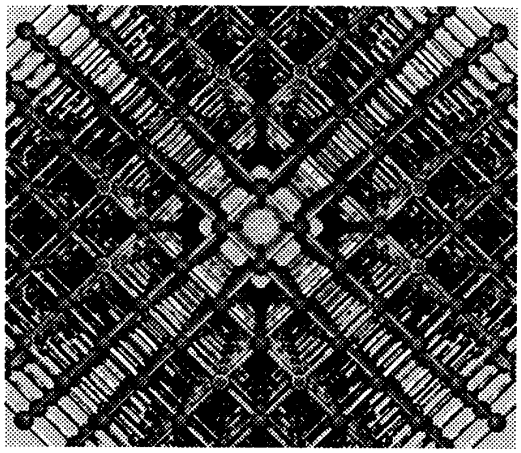

Figure 11: Stationary view of a blinking 3D lattice.

as transparency, polarization, magnetization or other physical properties permits results from other physical simulations to be used as part of the basic object models in REST-frame simulations.

When the *light sources* in ray-tracing are assigned with temporal properties, one can endeavor to simulate the effect of switching on and off the navigation radar on a fast spacecraft.[13] The spacetime tracking algorithm we developed for camera control in animation may be applied in the solving of spacetime navigation problems.

The appropriate modeling of the time component in ray-tracing also provides the essential connection between space and time via light. It becomes natural to simulate subjects of large physical, and thus temporal, scale. For example, it is possible to apply a 4D recovery methodology to existing or future NASA large-scale astrophysics databases. Data derived from such 4D spacetime representations can be used for simulations from different perspectives, by extrapolating from the initial single view and giving, e.g. how an astrophysical event is perceived from different galaxies. Other members of this category include the exchange of Neptune images and control commands over a four light-hour channel between Voyager II and its home planet, and the evolution of the Crab nebula (M1) and its optical pulsar (the run-away "lighthouse"). The Crab nebula, more than 6500 light years distant with a diameter of about 10 light years, is a remnant of a supernova event which was recorded by Chinese chroniclers as a bright "guest star" in 1054 AD. Note how this rich information about space and time can be conveniently represented in our simulation framework.

[13] What is the strategy for conducting a radar-based navigation and search in a hostile situation? Notice that the spacecraft, the radar beam, and the laser weapon all have comparable speeds — quite a departure from the conventional setting of the submarine, sonar and missile.

7 Conclusions

Our work may enhance the field of scientific visualization in the following ways:

1. It calls our attention to the temporal treatment of ray-tracing. A framework is presented that integrates the space and time dimensions by modeling the ray in ray-tracing as a spacetime concept.

2. It visually subjects us to the "abnormalities" when we implement the finite light-speed in ray-tracing. Consecutive wavefronts from flashes of light propagate as rings on an object's surface; synchronized blinking lights *appear* to send signals out of step, and above all, time dilation in the relativistic thought experiment is shown to depend on the condition of observation.

3. It distinctly illustrates the interplay of the imag*ing* process and the imag*ed* physical events in producing the final images. Our comprehensive 4D survey and empirical method reveals a richly detailed physical reality which the mathematical language of thought experiment does not directly provide.

We hope that our evolving spacetime visualization software will contribute to the exploration and understanding of the universe in which space and time are interwoven.

Acknowledgments

We would like to thank our reviewers for their valuable comments. We are also grateful to Michael Wu for his constant assistance. Nathan Loofbourrow's participation

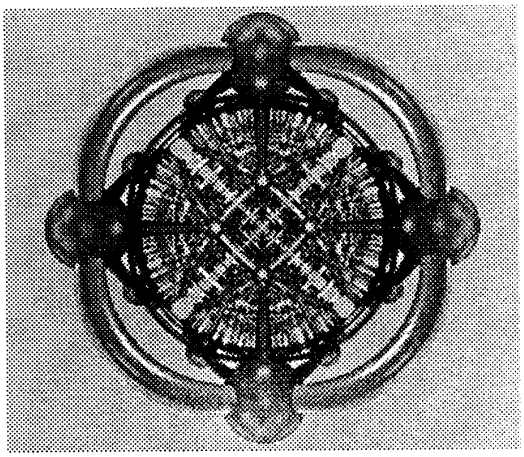

Figure 12: Blinking lattice moving at 0.99c towards the camera.

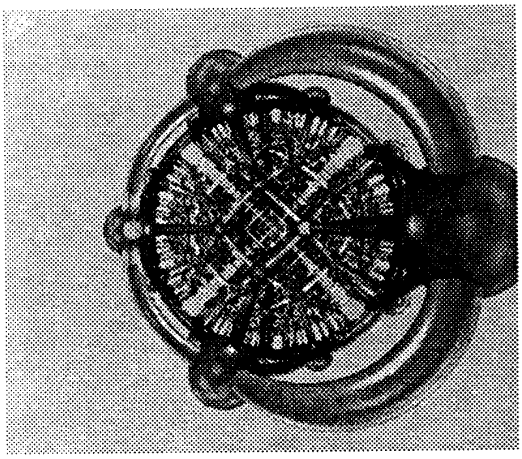

Figure 13: Blinking lattice moving at 0.99c with camera slightly off the lattice's central axis (T=0.0).

in the early stage of this research is remembered with gratitude.

References

[1] Andrew S. Glassner. *An Introduction to Ray-Tracing*. Academic Press Limited, 1989.

[2] Robert Goldstein and Roger Nagel. 3-D visual simulation. *Simulation*, page 25, 1971.

[3] Ping-Kang Hsiung and Robert H. P. Dunn. Visualizing relativistic effects in spacetime. In *Proceedings of the Supercomputing '89 Conference*, Nov. 13-17, 1989.

[4] Ping-Kang Hsiung and Robert H. Thibadeau. Spacetime visualization of relativistic effects. In *ACM 1990 Computer Science Conference*, Feb. 20-22, 1990.

[5] Ping-Kang Hsiung, Robert H. Thibadeau, Christopher B. Cox, and Robert H. P. Dunn. Doppler color shift in relativistic image synthesis. In *International Conference on Information Technology (Tokyo, Japan)*, October 1990.

[6] Ping-Kang Hsiung, Robert H. Thibadeau, Christopher B. Cox, Robert H.P. Dunn, Paul Andrew Olbrich, and Michael Wu. Wide-band relativitsic Doppler effect visualization. In *Visualization 90*, Oct. 1990.

[7] Ping-Kang Hsiung, Robert H. Thibadeau, and Michael Wu. T-Buffer: Fast visualization of relativistic effects in spacetime. In *1990 Symposium on Interactive 3D Graphics*, March 18-21, 1990.

[8] C. Møller. *The Theory of Relativity*. Clarendon Press, Oxford, 1972.

[9] MAGI. A geometric description technique suitable for computer analysis of both nuclear and conventional vulnerability of armored military vehicles. Technical report, MAGI, 1967.

[10] Roger Penrose. The apparent shape of a relativistically moving sphere. *Proceedings of the Cambridge Philosophical Society*, 55:137–9, July 29 1958.

[11] Robert Resnick. *Introduction to Special Relativity*. Rensselaer Polytechnic Institute, 1968.

[12] Edwin Taylor and John Wheeler. *Spacetime Physics*. M.I.T. / Princeton, 1966.